Vol 450|13 December 2007|doi:10.1038/nature06386

LETTERS

Reconstitution of a microtubule plus-end tracking system *in vitro*

Peter Bieling[1]*, Liedewij Laan[2]*, Henry Schek[1], E. Laura Munteanu[2], Linda Sandblad[1], Marileen Dogterom[2], Damian Brunner[1] & Thomas Surrey[1]

The microtubule cytoskeleton is essential to cell morphogenesis. Growing microtubule plus ends have emerged as dynamic regulatory sites in which specialized proteins, called plus-end-binding proteins (+TIPs), bind and regulate the proper functioning of microtubules[1–4]. However, the molecular mechanism of plus-end association by +TIPs and their ability to track the growing end are not well understood. Here we report the *in vitro* reconstitution of a minimal plus-end tracking system consisting of the three fission yeast proteins Mal3, Tip1 and the kinesin Tea2. Using time-lapse total internal reflection fluorescence microscopy, we show that the EB1 homologue Mal3 has an enhanced affinity for growing microtubule end structures as opposed to the microtubule lattice. This allows it to track growing microtubule ends autonomously by an end recognition mechanism. In addition, Mal3 acts as a factor that mediates loading of the processive motor Tea2 and its cargo, the Clip170 homologue Tip1, onto the microtubule lattice. The interaction of all three proteins is required for the selective tracking of growing microtubule plus ends by both Tea2 and Tip1. Our results dissect the collective interactions of the constituents of this plus-end tracking system and show how these interactions lead to the emergence of its dynamic behaviour. We expect that such *in vitro* reconstitutions will also be essential for the mechanistic dissection of other plus-end tracking systems.

Microtubules are polar, dynamic tubulin polymers that have a variety of functions in eukaryotic cells[5]. The dynamics and the spatial organization of microtubules are regulated by several highly conserved microtubule-associated proteins. An important class of these proteins, called +TIPs, accumulates selectively at growing microtubule plus ends in living cells. A wealth of fluorescence microscopy studies in various organisms have identified numerous +TIPs that belong to conserved subfamilies: CLIP-170 (ref. 6), APC (ref. 7), EB1 (ref. 8), CLASPs (ref. 9), p150 (ref. 10) and spectraplakins[11]. In the fission yeast *Schizosaccharomyces pombe*, classical genetics combined with real-time fluorescence microscopy[12] demonstrated that multiple aspects of cellular organization depend on a defined distribution of microtubules[13,14]. This distribution is mediated by, among others, three +TIPs: the EB1 homologue Mal3 (ref. 15), the Clip170 homologue Tip1 (ref. 16) and the kinesin Tea2 (refs 17, 18). A hierarchy of molecular events required for plus-end tracking has been established from observations inside living yeast cells: the motor Tea2 and its putative cargo Tip1 move along the microtubule lattice towards its growing plus ends, where they accumulate[17,19]. Efficient recruitment to microtubules and the plus-end accumulation of Tea2 and Tip1 depend on the presence of Mal3, which itself tracks the microtubule plus ends independently of Tea2 and Tip1 (refs 15, 17, 19). It is not yet known whether additional factors or post-translational modifications are required, or whether Mal3, Tea2 and Tip1 constitute a minimal system that is sufficient to show plus-end tracking. In fact, a mechanistic understanding of plus-end tracking is still missing, in part because of the lack of an *in vitro* assay in which plus-end tracking can be reconstituted with a minimal set of pure components[20].

Here we reconstitute microtubule plus-end tracking of the three purified proteins, namely Mal3, Tea2 and Tip1, *in vitro*. We observed +TIPs and dynamic microtubules on chemically functionalized surfaces by two-colour total internal reflection fluorescence (TIRF) microscopy[21] (Fig. 1a). We first studied the three +TIPs individually and then in various combinations with fluorescently labelled and unlabelled +TIPs.

Only one of the three proteins, the EB1 homologue Mal3, was able to bind efficiently to dynamic microtubules in the absence of the others. Alexa 488-labelled Mal3 selectively accumulated at growing microtubule ends at considerable ionic strength (Fig. 1b) over a wide range of protein concentrations (Supplementary Fig. 1a). Movie sequences and the corresponding kymographs (time–space plots), revealed that Mal3 was tracking both the fast-growing plus ends and the more slowly growing minus ends (Fig. 1c). However, Mal3 did not accumulate at the ends of depolymerizing microtubules (Fig. 1c and Supplementary Movie 1) or static microtubules (Supplementary Fig. 2a). Selective tracking of free, polymerizing microtubule ends is therefore an inherent property of Mal3. Mal3–Alexa 488 also bound weakly along the entire length of microtubules (Fig. 1b, c), a behaviour that was enhanced at lower ionic strength (Supplementary Fig. 1a). This binding might reflect the previously shown preferential association of Mal3 with the lattice seam of Taxol-stabilized microtubules[22].

Two fundamentally different molecular mechanisms can be envisaged for how Mal3 accumulates at the growing microtubule end. Mal3 could co-polymerize in a complex with tubulin to the growing microtubule end, and subsequently be released. Alternatively, instead of binding to free tubulin, Mal3 could recognize a characteristic structural feature at the microtubule end. This structural feature could either be a collective property of several tubulin subunits such as the previously observed protofilament sheet[23] or a property of individual tubulin dimers that are in a GTP-bound versus a GDP-bound state[24]. To distinguish between a co-polymerization mechanism and an end-recognition mechanism, we measured the spatial distribution of Mal3 along microtubule plus ends that were growing in the presence of various tubulin concentrations but a constant Mal3 concentration.

Increased microtubule growth velocities resulting from increased tubulin concentrations led to a more comet-shaped accumulation of

[1]European Molecular Biology Laboratory, Cell Biology and Biophysics Unit, Meyerhofstrasse 1, 69117 Heidelberg, Germany. [2]FOM Institute for Atomic and Molecular Physics (AMOLF), Kruislaan 407, 1098 SJ Amsterdam, The Netherlands.
*These authors contributed equally to this work.

Mal3–Alexa 488 at growing microtubule plus ends (Fig. 2a). Averaged fluorescence intensity profiles of Mal3–Alexa 488 comets demonstrated that after an initial peak in fluorescence the signal decreased exponentially towards the basal lattice signal (Fig. 2a). The peak fluorescence of Mal3 was largely insensitive to changes in the tubulin/Mal3 ratio (Fig. 2b). This argues against a simple co-polymerization mechanism, because such a mechanism would lead to peak signals that varied with the tubulin/Mal3 ratio. Furthermore, gel-filtration experiments showed that Mal3 does not bind to unpolymerized tubulin (Supplementary Fig. 3a). This agrees with the observation that the amount of Mal3 binding along the microtubule lattice is also independent of the tubulin concentration (Fig. 2b). Together these data support a mechanism in which Mal3 tracks microtubule ends by recognizing a structural feature.

The characteristic comet tail length obtained from exponential fits to the decays of the averaged Mal3 fluorescence intensity profiles increased linearly with the microtubule growth velocity (Fig. 2c). This suggests that microtubule ends are decorated with Mal3 for a characteristic time of about 8 s, independently of microtubule growth velocity (Fig. 2d). In contrast, the dwell time of individual Mal3–Alexa 488 molecules at growing microtubule plus ends, measured with greater temporal resolution under single-molecule imaging conditions, was only 0.282 ± 0.003 s (Fig. 2e and Supplementary Fig. 4). This indicates that individual Mal3 molecules turn over rapidly on a plus-end-specific structure that has a lifetime of about 8 s before it transforms into a normal microtubule lattice structure. A similarly fast turnover of Mal3 was also observed *in vivo*[19].

In contrast to Mal3, green fluorescent protein (GFP)-tagged Tip1 and Alexa 488-labelled Tea2 did not bind significantly to the microtubules in conditions under which selective end tracking of Mal3 was observed (Fig. 3a). Under single-molecule imaging conditions, however, rare interactions of the kinesin Tea2 with the microtubule could be observed at low ionic strengths with the use of higher frame rates. A gaussian fit to the velocity distribution yielded a mean velocity of $4.8 \pm 0.3\ \mu m\ min^{-1}$, and a single-exponential fit to the '1 − cumulative probability' distribution of the measured run lengths yielded an average run length of $0.73 \pm 0.01\ \mu m$ (Fig. 3b).

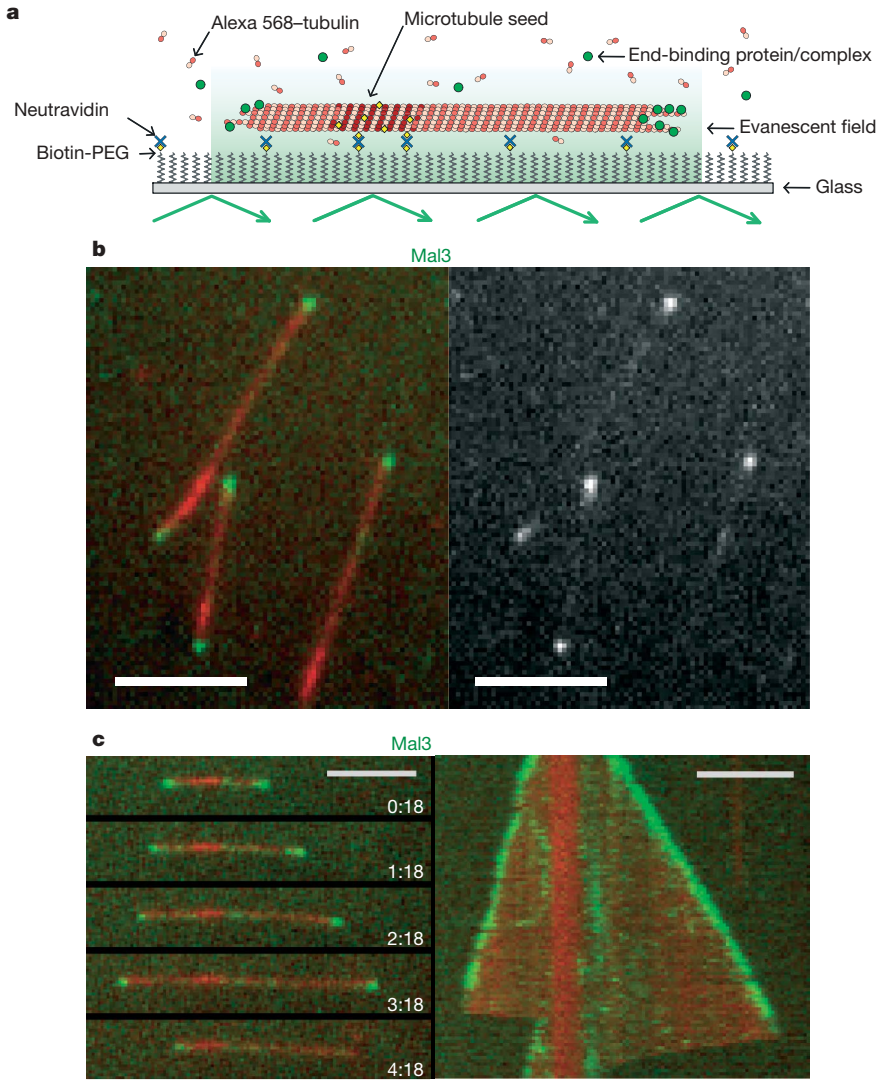

Figure 1 | Tracking of growing microtubule ends by Mal3 *in vitro*. **a**, Diagram of the experimental setup. Dynamic microtubules were grown in the presence of free Alexa 568-labelled tubulin and fluorescently labelled +TIPs from short stabilized microtubule seeds attached to a PEG-passivated glass surface by means of biotin-neutravidin links. Bright microtubule seeds, dim (non-biotinylated) microtubules extending from the seeds, and +TIPs were observed by TIRF microscopy in the evanescent field close to the glass surface. **b**, Overlaid TIRF images of Mal3–Alexa 488 (green) and dynamic Alexa 568-labelled microtubules (red) (left), and for comparison the image of Mal3–Alexa 488 alone (right). **c**, Time sequence of overlaid images of Mal3–Alexa 488 (green) and a dynamic Alexa 568-labelled microtubule (red) taken at the indicated times in minutes:seconds (left), and the corresponding kymograph of the same microtubule (right). Mal3 was used at 200 nM in all end-tracking experiments, unless otherwise stated. The kymograph displays a period of 5 min. Scale bars, 5 μm.

Because Tea2 binds *in vivo*[15] and *in vitro* (Supplementary Fig. 3b) to Tip1, and because the motor might be auto-inhibited without its putative cargo, we tested whether Tip1 could enhance the binding of Tea2–Alexa 488 to dynamic microtubules. However, this was not the case (Fig. 3a and Supplementary Movie 2).

In vivo, the presence of Mal3 is needed for plus-end tracking of Tea2 and Tip1 (refs 15, 17, 19). Using our *in vitro* approach, we examined whether the autonomous plus-end tracking protein Mal3 is sufficient to mediate microtubule plus-end tracking of the processive motor Tea2 and its cargo Tip1. In the presence of Mal3 and Tip1, Tea2–Alexa 488 now strongly accumulated at growing microtubule plus ends (Fig. 4a and Supplementary Movie 3). No accumulation of Tea2–Alexa 488 was visible at growing minus ends (Fig. 4a) or depolymerizing ends (Supplementary Fig. 1b). Furthermore, Tea2–Alexa 488 speckles appeared along the microtubule lattice and moved towards the plus end (Fig. 4a and Supplementary Movie 3). The speed of these particles was on average $9.8 \pm 2.9\ \mu m\ min^{-1}$ and therefore 4.4-fold faster than the velocity of microtubule growth ($2.2 \pm 0.3\ \mu m\ min^{-1}$; Fig. 4b). Tip1–GFP moved similarly along the microtubule lattice and also tracked growing microtubule plus ends (Fig. 4c and Supplementary Movie 4), but not depolymerizing ends (Supplementary Fig. 1b) or the ends of static microtubules (Supplementary Fig. 2b). Mal3–Alexa 488, in contrast, was not observed to move along the microtubule to the same extent as Tea2 and Tip1 (Fig. 4d and Supplementary Movie 5). These observations very closely mimic the situation *in vivo*[15,17,19].

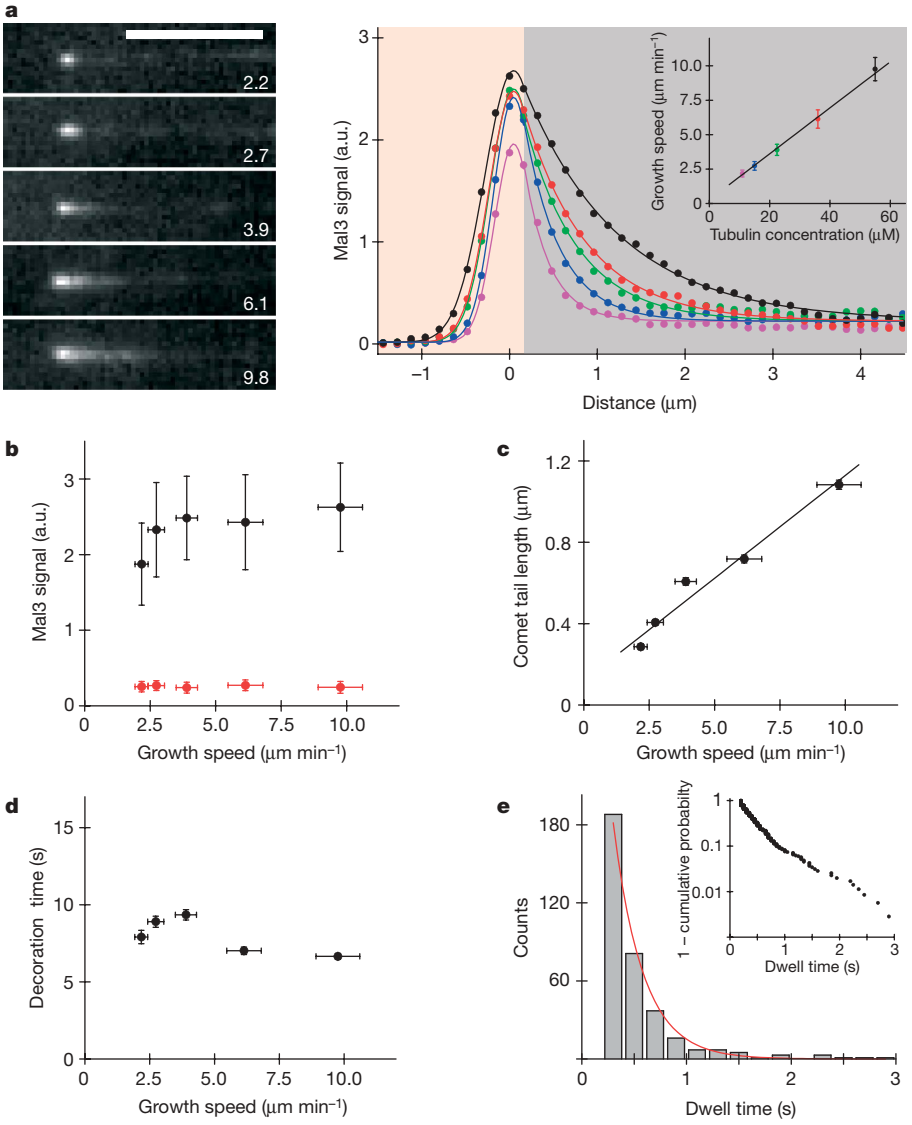

Figure 2 | Mechanism of plus-end tracking by Mal3. a, Images of individual Mal3–Alexa 488 comets at the indicated growth velocities (in $\mu m\ min^{-1}$) (left) and averaged intensity profiles of the comets (right). The Mal3–Alexa 488 concentration was 200 nM. The data (dots) were fitted (lines) using gaussian (pink area) and exponential (grey area) functions (Supplementary Methods). The inset shows the dependence of the growth velocities on tubulin concentrations. Error bars indicate s.d. **b**, The Mal3–Alexa 488 signal at the peak of the Mal3 comet (black symbols) as obtained from the averaged intensity profiles, and the signal on the microtubule lattice behind the comet (red symbols) as quantified separately from intensity line scans. Error bars indicate the s.d. of the maximum tip intensity and the s.d. of the averaged line scans for the lattice intensity. **c**, Mal3 comet tail lengths as obtained from single-exponential fits to the averaged intensity profiles. Error bars indicate standard errors as obtained from the exponential fits. **d**, The characteristic decoration time of the Mal3 signal in the Mal3 comet tail at different microtubule growth speeds as obtained by dividing the comet tail length by the microtubule growth speed. Errors were calculated by error propagation. **e**, Histogram of dwell times of single Mal3–Alexa 488 events at growing microtubule plus ends. The inset shows the '1 − cumulative probability' distribution of dwell times. The characteristic dwell time and its standard error was obtained from a fit to this distribution (red line, see Supplementary Methods). The Mal3–Alexa 488 concentration was 1 nM.

Gel filtrations demonstrated that in solution Mal3, Tea2 and Tip1 exist as a stable ternary complex (Fig. 4e). It is therefore most likely that the formation of this complex is required for efficient binding of Tea2–Tip1 to the microtubule. However, the three proteins do not behave in the same way once bound to the microtubule. Imaging the movements of the three proteins on the microtubule lattice with greater temporal resolution showed that Tip1–GFP and Alexa 647-labelled Tea2 co-migrate (Supplementary Fig. 5), indicating that Tea2 indeed transports Tip1. Consistent with this was our observation that the average run lengths for Tea2 and Tip1 were very similar, at 0.90 ± 0.01 and 1.10 ± 0.01 μm, respectively (Fig. 4f and Supplementary Fig. 6). In contrast, Mal3–Alexa 488 showed only short runs with an average run length of 0.29 ± 0.01 μm (Fig. 4f and Supplementary Fig. 6). This demonstrates that Mal3 is initially transported by Tea2, but dissociates shortly after a productive binding event.

We confirmed that Mal3-mediated recruitment of Tea2–Tip1 to the microtubule lattice requires the interaction of Mal3 with the amino-terminal extension of the kinesin Tea2 (ref. 25). Replacing full-length Tea2 with a construct lacking the N-terminal extension (ΔNTea2) abolished efficient binding of Tip1–GFP to the microtubule (Supplementary Fig. 7a). In addition, Mal3-mediated recruitment of the Tea2–Tip1 complex requires the presence of both Tea2 and Tip1. Tea2–Alexa 488 was hardly present on microtubules in the absence of Tip1 (Supplementary Fig. 7b) and Tip1–GFP was not significantly bound to microtubules in the absence of Tea2 (Supplementary Fig. 7c), whereas binding of Mal3–Alexa 488 to microtubules was unaffected in both cases (Supplementary Fig. 7d and data not shown). The results with the double combinations of proteins (Fig. 3a, right, and Supplementary Fig. 7b–d) exactly mimic the *in vivo* single-deletion mutants of *mal3*, *tea2* and *tip1* (refs 15, 17, 19).

Replacing ATP with ADP eliminated the efficient binding of Tea2–Alexa 488 along the microtubule lattice and the tracking of microtubule plus ends, despite the presence of all three proteins (Supplementary Fig. 7e and Supplementary Movie 6). Only a very weak fluorescence signal could be observed at growing microtubule ends, but without a preference for the plus or minus end (Supplementary Fig. 7e). This demonstrates that *in vitro* the processive motor activity of Tea2 is essential for efficient microtubule-end tracking of Tea2–Tip1 and also for their plus-end preference.

In living cells, single deletions of Mal3, Tea2 or Tip1 suggested that these three +TIPs mainly decrease the frequency of microtubule catastrophes without strongly affecting the other parameters of microtubule dynamic instability[15,16,18]. We tested the direct effects of Mal3 alone and of Mal3 with Tea2 and Tip1 on microtubule dynamics under conditions of selective end tracking. We imaged microtubules in the presence of unlabelled +TIPs by differential interference contrast microscopy. Similarly to the situation *in vivo*, neither Mal3 alone nor the combination of all three proteins had a strong effect on the growth and shrinkage velocities of microtubule plus ends (Supplementary Table 1). However, Mal3 alone increased the frequencies of catastrophes and rescues. The addition of Tea2–Tip1 counteracted these effects of Mal3 (Supplementary Table 1). These results show that especially the effect of Mal3 on the catastrophe frequency is different from what would be expected from the corresponding deletion *in vivo*. This is not surprising, because several other proteins not studied here are known to affect the catastrophe frequency[26,27]. By including these other modulators of microtubule dynamics in the future, our *in vitro* system promises also to lead to the identification of the more complex minimal system that reproduces physiological microtubule dynamics.

Thus, we have identified Mal3 as an autonomous tracking protein of growing microtubule ends *in vitro*. Mal3 most probably recognizes a structural feature at microtubule ends rather than co-polymerizing as a tubulin–Mal3 complex. As *in vivo*, the behaviour of Mal3 *in vitro* does not depend significantly on the presence of Tea2 or Tip1. Furthermore, we identified Mal3–Tea2–Tip1 as a minimal system producing plus-end tracking behaviour of Tea2 and Tip1 *in vitro*. This suggests that *in vivo* Tea2, Tip1 and Mal3 may also work as a

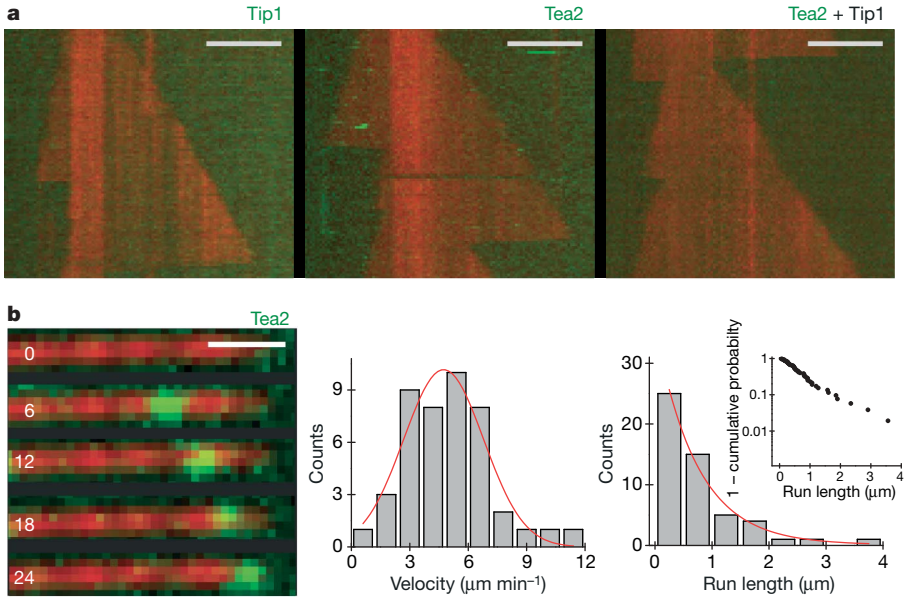

Figure 3 | Tea2 and Tip1 individually and in combination do not track microtubule ends. **a**, Kymographs of Tip1–GFP (left), Tea2–Alexa 488 (middle), and Tea2–Alexa 488 together with Tip1 (right) (labelled +TIPs in green) on dynamic Alexa 568-labelled microtubules (red). The sensitivity for GFP and Alexa 488 detection was strongly increased in comparison with that in Fig. 1b. Concentrations were 50 nM for Tip1 and 8 nM for Tea2 in all end-tracking experiments unless otherwise stated. The kymographs display a period of 5 min. Scale bars, 5 μm. **b**, Time sequence of TIRF images of a processive run of a single Tea2–Alexa 488 (see also Supplementary Fig. 8) moving on a stable Alexa 568-labelled microtubule, taken at the indicated times in seconds (left). Scale bar, 1 μm. The Tea2–GFP concentration was 0.5 nM. Histograms of velocities (centre) and run lengths (right) of single Tea2–Alexa 488 runs are shown; the inset shows the '1 – cumulative probability' distribution of run lengths. The red lines show a gaussian fit to the velocity distribution (centre) and a single-exponential fit to the '1 – cumulative probability' distribution of run lengths (right) (see Supplementary Methods).

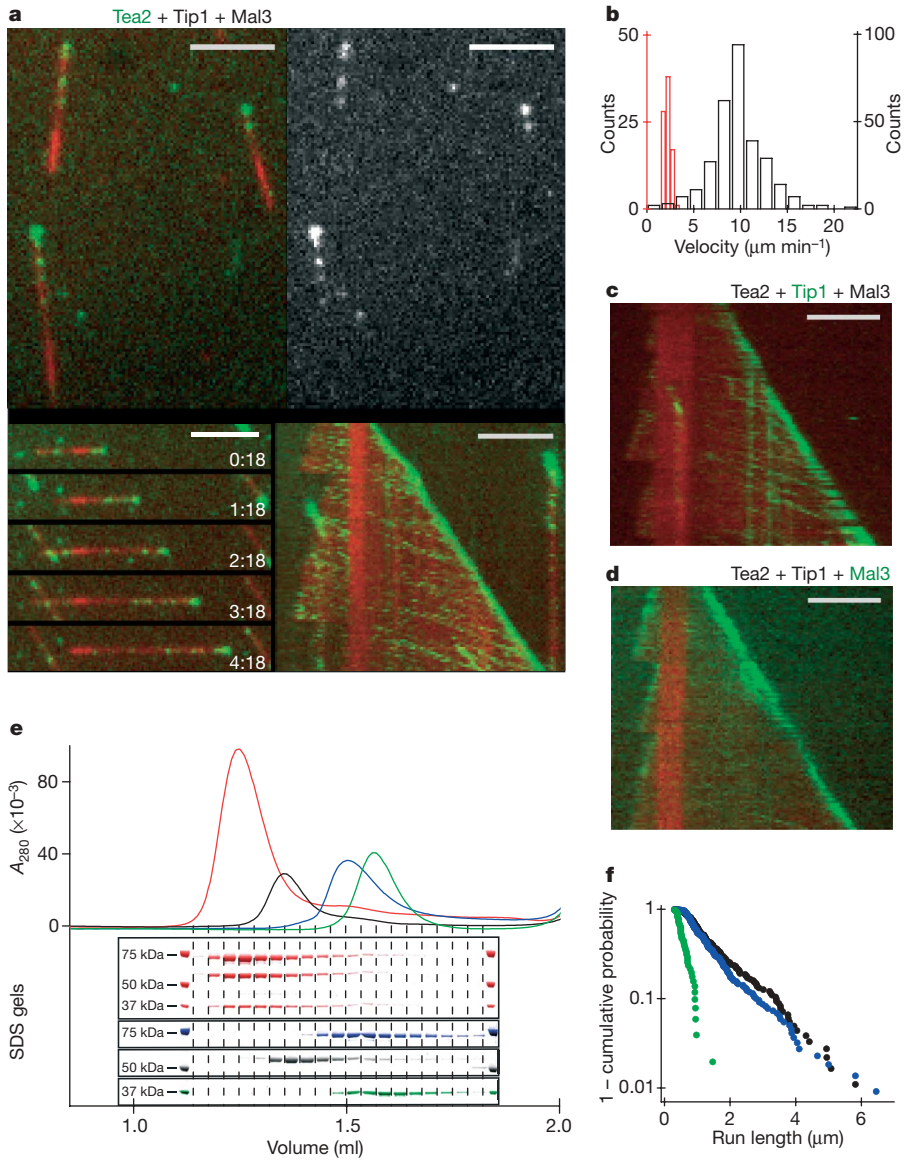

Figure 4 | Efficient microtubule plus-end tracking of Tea2–Tip1 in the presence of Mal3. a, Overlaid TIRF images showing Tea2–Alexa 488 (green) and Alexa 568-labelled microtubules (red) in the presence of the two other +TIPs (top left), and for comparison an image with the signal of only Tea2–Alexa 488 (top right). Bottom left, time sequence of images (at the times shown, in minutes:seconds); bottom right, the corresponding kymograph. Protein concentrations for Mal3 are as in Fig. 1 and for Tea2 and Tip1 as in Fig. 3a. Kymographs display periods of 5 min. Scale bars, 5 μm. **b**, Histograms of the velocities of microtubule plus-end growth (red, left axis) and Tea2–Alexa 488 speckle movement along the microtubule lattice (black, right axis). The increased velocity of Tea2 speckles in comparison with single Tea2 molecules (Fig. 3b) is mostly a consequence of an increased temperature. **c**, Kymograph showing Tip1–GFP in the presence of Tea2 and Mal3. **d**, Kymograph showing Mal3–Alexa 488 (green) in the presence of Tea2 and Tip1. The signal intensity can be directly compared with Fig. 1b. **e**, Gel filtrations of Mal3, Tea2 and Tip1: elution profiles and SDS gels of the corresponding eluted fractions of individual runs of Mal3 alone (green), Tea2 alone (blue), Tip1 alone (black) and an equimolar mixture of all three +TIPs (red). **f**, Run-length distribution of Mal3–Alexa 488 (green), Tip1–GFP (black) and Tea2–Alexa 647 (blue) moving along the microtubule lattice, always in the presence of the other two +TIPs. Concentrations were 100 nM Mal3, 50 nM Tip1 and 8 nM Tea2.

microtubule plus-end tracking system, independently of other +TIPs. However, *in vivo* part of the Mal3 pool might simultaneously function in 'parallel' end tracking systems. The role of Mal3 as a loading factor of Tea2–Tip1 involves the initial formation of a ternary complex that promotes productive encounters of Tea2–Tip1 with the microtubule lattice. Tip1 is subsequently transported by the processive motor Tea2, whereas Mal3 rapidly dissociates and is transported for only short distances.

Our *in vitro* system provides a powerful new tool to test the proposed mechanisms for microtubule end targeting of different +TIPs[20,28,29] and to analyse the interplay between plus-end tracking and the dynamic properties of microtubules that are ultimately responsible for the morphogenetic function of the microtubule cytoskeleton.

METHODS SUMMARY

Protein biochemistry. Proteins were expressed, purified and labelled as described in Supplementary Methods.

Surface chemistry. Glass coverslips were cleaned, silanized and functionalized with poly(ethylene glycol) (PEG) as described[30], and treated with *N*-hydroxysuccinimido-biotin. The biotin-PEG-functionalized slides were washed, spin-dried and stored at 4 °C. To generate passivated glass, poly(L-lysine)-PEG was dried on a glass surface and then washed extensively.

End-tracking assay. Brightly labelled, short GMP-CPP microtubules (containing 20% Alexa 568-labelled tubulin and 7.7% biotinylated tubulin) were attached by means of neutravidin to a biotin-PEG-functionalized coverslip of a flow chamber (Supplementary Methods). With the use of a custom TIRF microscopy system, dynamic microtubules and +TIPs either tagged with GFP or labelled with Alexa fluorophores were observed in the presence of 11 μM dimly labelled tubulin (containing 6.7% Alexa 568-labelled tubulin) in assay

buffer (80 mM K-PIPES pH 6.8, 85 mM KCl, 4 mM $MgCl_2$, 1 mM GTP, 1 mM EGTA, 10 mM 2-mercaptoethanol and 2 mM MgATP or MgAMP-PNP or 5 mM MgADP) containing 0.1% methylcellulose (4,000 cP; Sigma) and an oxygen scavenger system. Unless stated otherwise, we kept the final concentrations of the labelled and unlabelled +TIP proteins constant at 200 nM Mal3, 50 nM Tip1 and 8 nM Tea2. These protein concentrations were chosen after systematic variation of concentrations to allow the easy visualization of both end tracking and transport along microtubules. The temperature was 30 °C.

Data analysis. The growth trajectories of microtubules and walking tracks of Tea2–Tip1 speckles were analysed with kymographs. Single-molecule motility was analysed with kymographs and by automated particle tracking implemented in a custom software environment. To analyse the shape of Mal3 comets, line profiles of the fluorescence intensity of Mal3–Alexa 488 at growing microtubule plus ends were aligned and averaged. An exponential fit to the tail of the profile was then used to quantify the decay of the signal.

Detailed methods are described in Supplementary Methods.

Received 18 September; accepted 17 October 2007.
Published online 2 December 2007.

1. Schuyler, S. C. & Pellman, D. Microtubule 'plus-end-tracking proteins': The end is just the beginning. *Cell* **105,** 421–424 (2001).
2. Mimori-Kiyosue, Y. & Tsukita, S. 'Search-and-capture' of microtubules through plus-end-binding proteins (+TIPs). *J. Biochem.* **134,** 321–326 (2003).
3. Wittmann, T. & Desai, A. Microtubule cytoskeleton: a new twist at the end. *Curr. Biol.* **15,** R126–R129 (2005).
4. Akhmanova, A. & Hoogenraad, C. C. Microtubule plus-end-tracking proteins: mechanisms and functions. *Curr. Opin. Cell Biol.* **17,** 47–54 (2005).
5. Desai, A. & Mitchison, T. J. Microtubule polymerization dynamics. *Annu. Rev. Cell Dev. Biol.* **13,** 83–117 (1997).
6. Perez, F., Diamantopoulos, G. S., Stalder, R. & Kreis, T. E. CLIP-170 highlights growing microtubule ends *in vivo*. *Cell* **96,** 517–527 (1999).
7. Mimori-Kiyosue, Y., Shiina, N. & Tsukita, S. Adenomatous polyposis coli (APC) protein moves along microtubules and concentrates at their growing ends in epithelial cells. *J. Cell Biol.* **148,** 505–518 (2000).
8. Mimori-Kiyosue, Y., Shiina, N. & Tsukita, S. The dynamic behavior of the APC-binding protein EB1 on the distal ends of microtubules. *Curr. Biol.* **10,** 865–868 (2000).
9. Akhmanova, A. *et al.* Clasps are CLIP-115 and -170 associating proteins involved in the regional regulation of microtubule dynamics in motile fibroblasts. *Cell* **104,** 923–935 (2001).
10. Vaughan, P. S., Miura, P., Henderson, M., Byrne, B. & Vaughan, K. T. A role for regulated binding of $p150^{Glued}$ to microtubule plus ends in organelle transport. *J. Cell Biol.* **158,** 305–319 (2002).
11. Kodama, A., Karakesisoglou, I., Wong, E., Vaezi, A. & Fuchs, E. ACF7: an essential integrator of microtubule dynamics. *Cell* **115,** 343–354 (2003).
12. Ding, D. Q., Chikashige, Y., Haraguchi, T. & Hiraoka, Y. Oscillatory nuclear movement in fission yeast meiotic prophase is driven by astral microtubules, as revealed by continuous observation of chromosomes and microtubules in living cells. *J. Cell Sci.* **111,** 701–712 (1998).
13. Hayles, J. & Nurse, P. A journey into space. *Nature Rev. Mol. Cell Biol.* **2,** 647–656 (2001).
14. Brunner, D. & Nurse, P. New concepts in fission yeast morphogenesis. *Phil. Trans. R. Soc. Lond. B* **355,** 873–877 (2000).
15. Busch, K. E. & Brunner, D. The microtubule plus end-tracking proteins mal3p and tip1p cooperate for cell-end targeting of interphase microtubules. *Curr. Biol.* **14,** 548–559 (2004).
16. Brunner, D. & Nurse, P. CLIP170-like tip1p spatially organizes microtubular dynamics in fission yeast. *Cell* **102,** 695–704 (2000).
17. Browning, H., Hackney, D. D. & Nurse, P. Targeted movement of cell end factors in fission yeast. *Nature Cell Biol.* **5,** 812–818 (2003).
18. Browning, H. *et al.* Tea2p is a kinesin-like protein required to generate polarized growth in fission yeast. *J. Cell Biol.* **151,** 15–28 (2000).
19. Busch, K. E., Hayles, J., Nurse, P. & Brunner, D. Tea2p kinesin is involved in spatial microtubule organization by transporting tip1p on microtubules. *Dev. Cell* **6,** 831–843 (2004).
20. Carvalho, P., Tirnauer, J. S. & Pellman, D. Surfing on microtubule ends. *Trends Cell Biol.* **13,** 229–237 (2003).
21. Axelrod, D. Total internal reflection fluorescence microscopy in cell biology. *Traffic* **2,** 764–774 (2001).
22. Sandblad, L. *et al.* The *Schizosaccharomyces pombe* EB1 homolog Mal3p binds and stabilizes the microtubule lattice seam. *Cell* **127,** 1415–1424 (2006).
23. Chretien, D., Fuller, S. D. & Karsenti, E. Structure of growing microtubule ends: two-dimensional sheets close into tubes at variable rates. *J. Cell Biol.* **129,** 1311–1328 (1995).
24. Drechsel, D. N. & Kirschner, M. W. The minimum GTP cap required to stabilize microtubules. *Curr. Biol.* **4,** 1053–1061 (1994).
25. Browning, H. & Hackney, D. D. The EB1 homolog Mal3 stimulates the ATPase of the kinesin Tea2 by recruiting it to the microtubule. *J. Biol. Chem.* **280,** 12299–12304 (2005).
26. West, R. R., Malmstrom, T., Troxell, C. L. & McIntosh, J. R. Two related kinesins, klp5+ and klp6+, foster microtubule disassembly and are required for meiosis in fission yeast. *Mol. Biol. Cell* **12,** 3919–3932 (2001).
27. Ohkura, H., Garcia, M. A. & Toda, T. Dis1/TOG universal microtubule adaptors—one MAP for all? *J. Cell Sci.* **114,** 3805–3812 (2001).
28. Tirnauer, J. S., Grego, S., Salmon, E. D. & Mitchison, T. J. EB1–microtubule interactions in *Xenopus* egg extracts: role of EB1 in microtubule stabilization and mechanisms of targeting to microtubules. *Mol. Biol. Cell* **13,** 3614–3626 (2002).
29. Folker, E. S., Baker, B. M. & Goodson, H. V. Interactions between CLIP-170, tubulin, and microtubules: implications for the mechanism of Clip-170 plus-end tracking behavior. *Mol. Biol. Cell* **16,** 5373–5384 (2005).
30. Lata, S. & Piehler, J. Stable and functional immobilization of histidine-tagged proteins via multivalent chelator headgroups on a molecular poly(ethylene glycol) brush. *Anal. Chem.* **77,** 1096–1105 (2005).

Supplementary Information is linked to the online version of the paper at www.nature.com/nature.

Acknowledgements We thank M. Utz for technical assistance, protein purifications and cloning; J. Piehler for help with surface chemistry; I. Telley for help with data analysis; M. Braun and A. Seitz for helping to initiate this project; H. Besir for protein purifications; R. Santarella and S. Kandels-Lewis for cloning; G. Stier for the gift of pETM-Z; Y. Kalaidzidis and Transinsight GMBH for the gift of the PLUK MT beta version used to track moving particles; and G. Brouhard for additional help with the software. T.S. acknowledges support from the German Research Foundation (DFG), T.S. and M.D. from the European Commission (STREP Active Biomics), H.S. from EMBO, D.B. and M.D. from the Human Frontier Science Program, and M.D. from the 'Stichting voor Fundamenteel Onderzoek der Materie (FOM-NWO)'.

Author Information Reprints and permissions information is available at www.nature.com/reprints. Correspondence and requests for materials should be addressed to T.S. (surrey@embl.de), D.B. (brunner@embl.de) or M.D. (dogterom@amolf.nl).